

# Model-Independent Determination of CP Violation from Angular Distributions in Higgs Boson Decays to WW and ZZ at the Photon Collider

P.Nieźurawski, A.F.Żarnecki

*Institute of Experimental Physics, Warsaw University Hoża 69, 00-681 Warszawa, Poland*

M.Krawczyk

*Institute of Theoretical Physics, Warsaw University Hoża 69, 00-681 Warszawa, Poland*

October 21, 2004

## Abstract

The model-independent determination of the Higgs-boson CP properties at the Photon Collider at TESLA has been studied in detail, for masses between 200 and 350 GeV, using realistic luminosity spectra and detector simulation. We consider a generic model with the CP violating Higgs tensor couplings to gauge bosons. We introduce a new variable describing angular distributions of the secondary WW and ZZ decay products which is very sensitive to the CP properties of the Higgs-boson. Understanding of the detector performance turns out to be crucial, as the influence of the acceptance corrections is similar to the effects of CP violation. From the combined measurement of invariant mass distributions and various angular distributions the phase describing a CP violation can be determined to about 50 mrad after one year of Photon Collider running.

## 1 Introduction

The physics potential of a Photon Collider [1] is very rich and complementary to the physics program of the  $e^+e^-$  and hadron-hadron colliders. It is an ideal place to study the mechanism of the electroweak symmetry breaking (EWSB) and the properties of the Higgs-boson.

In paper [2] we performed a realistic simulation of the Standard Model (SM) Higgs-boson production at the Photon Collider for  $W^+W^-$  and  $ZZ$  decay channels, for Higgs-boson masses above 150 GeV. From the combined analysis of  $W^+W^-$  and  $ZZ$  invariant mass distributions the  $\gamma\gamma$  partial width of the Higgs boson,  $\Gamma_{\gamma\gamma}$ , can be measured with an accuracy of 3 to 8% and the phase of  $\gamma\gamma \rightarrow h$  amplitude,  $\phi_{\gamma\gamma}$ , with an accuracy between 30 and 100 mrad. In paper [3] we extended this analysis to the generalised Standard Model-like scenario  $B_h$  of the Two Higgs Doublet Model II, 2HDM(II), with and without CP-violation. In case of the solution

$B_h$  with a weak CP violation via  $H - A$  mixing, the mixing angle  $\Phi_{HA}$  can be constrained to about 100 mrad for low values of  $\tan\beta$ . We found that for a general 2HDM (II) with CP violation, only the combined analysis of LHC, LC and Photon Collider measurements allows for the precise determination of Higgs-boson couplings and of CP-violating  $H - A$  mixing angle [4].

In this paper our aim is to establish CP-property of the Higgs-boson in a generic model with a direct CP-violation. The measurement of the Higgs-boson properties at the Photon Collider at TESLA is studied in detail for masses between 200 and 350 GeV, using realistic luminosity spectra and detector simulation. The model with generic, CP-violating Higgs-boson couplings to vector bosons [5] leads to different angular distributions for a scalar- and pseudoscalar-type of couplings. From a combined analysis of invariant mass distributions and angular distributions of the  $W^+W^-$  and  $ZZ$  decay-products the CP-parity of the observed Higgs state can be determined independently on a production mechanism [6]. Results given in this paper supersede results presented in the second part of our earlier work [7].

## 2 Generic Higgs model with CP violating couplings

Following the analysis described in [5] we consider a generic model with a direct CP violation, with tensor couplings of a Higgs boson,  $\mathcal{H}$ , to  $ZZ$  and  $W^+W^-$  given by:

$$\begin{aligned} g_{\mathcal{H}ZZ} &= ig \frac{M_Z}{\cos\theta_W} \left( \lambda_H \cdot g^{\mu\nu} + \lambda_A \cdot \varepsilon^{\mu\nu\rho\sigma} \frac{(p_1 + p_2)_\rho (p_1 - p_2)_\sigma}{M_Z^2} \right), \\ g_{\mathcal{H}WW} &= ig M_W \left( \lambda_H \cdot g^{\mu\nu} + \lambda_A \cdot \varepsilon^{\mu\nu\rho\sigma} \frac{(p_1 + p_2)_\rho (p_1 - p_2)_\sigma}{M_W^2} \right), \end{aligned} \quad (1)$$

where  $p_1$  and  $p_2$  are the 4-momenta of the vector bosons. Contributions to gauge couplings with  $\lambda_H$  have a structure of the CP-even SM Higgs boson coupling,<sup>1</sup> whereas the ones with  $\lambda_A$  correspond to a general CP-odd coupling for the spin-0 boson. Coefficients  $\lambda_H$  and  $\lambda_A$  can be written as:

$$\begin{aligned} \lambda_H &= \lambda \cdot \cos\Phi_{CP}, \\ \lambda_A &= \lambda \cdot \sin\Phi_{CP}. \end{aligned} \quad (2)$$

The couplings of the Standard Model Higgs boson are reproduced for  $\lambda = 1$  and  $\Phi_{CP} = 0$  (i.e.  $\lambda_H = 1$  and  $\lambda_A = 0$ ). Below we will limit ourselves to  $\lambda \approx 1$  and  $|\Phi_{CP}| \ll 1$  region, corresponding to small deviation from the Standard Model coupling. However, we do not make any assumptions concerning Higgs-boson couplings to fermions and we allow for deviations from SM predictions in  $\Gamma_{\gamma\gamma}$  and  $\phi_{\gamma\gamma}$ . Therefore our results do not depend on the assumed Higgs-boson production mechanism and our approach can be considered as model-independent. To simplify the analysis, we only assume that the  $\mathcal{H}$  branching ratios to  $W^+W^-$  and  $ZZ$  are the same as in the Standard Model. No substantial deviations in the  $W^+W^-$  and  $ZZ$  branching ratios are expected unless Higgs-boson Yukawa couplings to up- or down-type fermions become very large. Possible small deviation in the branching ratios are equivalent to  $\Gamma_{\gamma\gamma}$  variation.

---

<sup>1</sup>Other possible CP-even tensor structure,  $(p_1 + p_2)^\mu (p_1 + p_2)^\nu$ , gives the angular distributions similar to that of the SM Higgs boson and therefore we will not consider this case separately.

### 3 Angular distributions for secondary decay products

Here we consider the Higgs boson decays to gauge bosons. The angular distributions of the secondary  $W^+W^-$  and  $ZZ$  decay products turn out to be very sensitive to the CP properties of the Higgs-boson [5]. Angular variables which can be used in the analysis are defined in Fig. 1. To test CP-properties of the Higgs-bosons the distributions of the polar angles  $\Theta_1$  and  $\Theta_2$  as well as the  $\Delta\phi$  distribution, where  $\Delta\phi$  is the angle between two  $Z$ - or two  $W$ -decay planes, are used. Here we propose to consider, instead of two-dimensional distribution in  $(\cos\Theta_1, \cos\Theta_2)$  the distribution in a new variable, defined as

$$\zeta = \frac{\sin^2\Theta_1 \cdot \sin^2\Theta_2}{(1 + \cos^2\Theta_1) \cdot (1 + \cos^2\Theta_2)}. \quad (3)$$

The  $\zeta$ -variable corresponds to the ratio of the angular distributions expected for the decay of a scalar and a pseudoscalar (in a limit  $M_{\mathcal{H}} \gg M_Z$ ) [5]. It proves to be very useful and complementary to  $\Delta\phi$  variable.

The angular distributions in  $\Delta\phi$  and  $\zeta$ , expected for a scalar ( $\Phi_{CP} = 0$ ) and a pseudoscalar ( $\Phi_{CP} = \frac{\pi}{2}$ ) higgs decays,  $\mathcal{H} \rightarrow ZZ \rightarrow l^+l^-jj$ , are compared in Fig. 2. They clearly distinguish between decays of scalar ( $H$ ) and pseudoscalar ( $A$ ) higgs. For the scalar higgs the distributions are almost flat in both  $\Delta\phi$  and  $\zeta$ . For the pseudoscalar case these two distributions have totally different character. From the measurement of one or other, or both of these distributions it's possible to establish the CP properties of the Higgs boson, even without taking into account the production mechanism.

Note, that the theoretical distribution of the higgs decay-angle  $\Theta_{\mathcal{H}}$  is expected to be flat both for scalar and pseudoscalar higgses, as this is characteristic to spin 0 particle. However, the measured  $\Theta_{\mathcal{H}}$  distributions for  $H$  and  $A$  decays can differ due to the different acceptance corrections and interference with a non-resonant background. Therefore, in the observed  $\Theta_{\mathcal{H}}$  distributions, as well as reconstructed  $\gamma\gamma$  invariant mass distributions for  $W^+W^-$  and  $ZZ$  decays, some sensitivity to the Higgs-boson couplings can show up.

### 4 Reconstruction of the angular distributions

Our analysis uses the CompAZ parametrisation [8] of the realistic luminosity spectra for a Photon Collider at TESLA. We assume that the centre-of-mass energy of colliding electron beams,  $\sqrt{s_{ee}}$ , is optimised for the production of a Higgs boson with a given mass. All results presented in this paper were obtained for an integrated luminosity corresponding to one year of the photon collider running. The total photon-photon luminosity increases from about  $600 \text{ fb}^{-1}$  for  $\sqrt{s_{ee}} = 305 \text{ GeV}$  (optimal beam energy choice for  $M_{\mathcal{H}} = 200 \text{ GeV}$ ) to about  $1000 \text{ fb}^{-1}$  for  $\sqrt{s_{ee}} = 500 \text{ GeV}$  ( $M_{\mathcal{H}} = 350 \text{ GeV}$ ).

Measurement of the angular distributions has been studied using the samples of  $ZZ$  events generated with the PYTHIA [9] and SIMDET [10] programs, as described in [2]. The resolutions of the reconstructed decay angles  $\Theta$  and  $\phi$ , for the scalar Higgs-boson with mass of 300 GeV

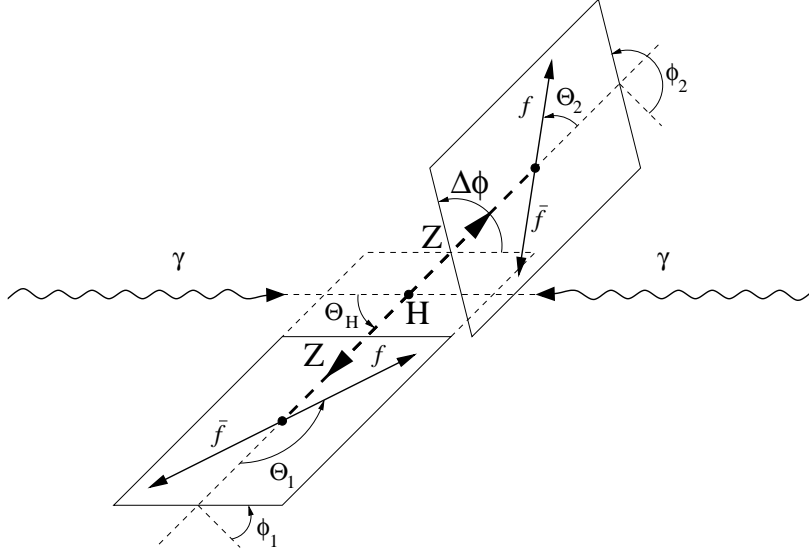


Figure 1: The definition of the polar angles  $\Theta_H$ ,  $\Theta_1$  and  $\Theta_2$ , and the azimuthal angles  $\phi_1$  and  $\phi_2$  for the process  $\gamma\gamma \rightarrow h \rightarrow ZZ \rightarrow 4f$ .  $\Delta\phi$  is the angle between two Z decay planes,  $\Delta\phi = \phi_2 - \phi_1$ . All polar angles are calculated in the rest frame of the decaying particle.

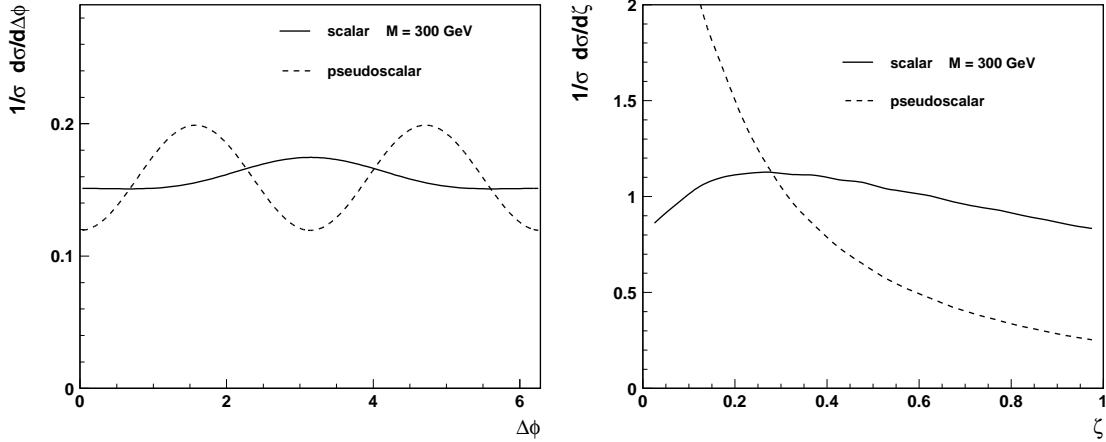


Figure 2: Normalised angular distributions in  $\Delta\phi$  (left plot) and  $\zeta$  (right plot), expected for scalar and pseudoscalar higgs decays  $H, A \rightarrow ZZ \rightarrow l^+l^-jj$ , for the higgs mass of 300 GeV.

(primary electron-beam energy of 209 GeV) are compared in Fig. 3 for the leptonic and hadronic  $Z$  decays.

A very good resolution is obtained for all considered distributions, nevertheless the measured angular distributions are strongly affected by the selection cuts used in the analysis. Because of the cut on the lepton and jet angles, applied to preserve a good mass resolution (see [2] for more details), we observe a significant loss of the selection efficiency for the events with lepton or jet emitted along the beam direction. Also the Durham jet algorithm used in the event reconstruction imposes constraints on the angular separation between leptons and jets. Both effects result in a highly non-uniform angular acceptance. The obtained selection efficiencies for  $\gamma\gamma \rightarrow ZZ \rightarrow l^+l^-jj$  events, as a function of the angle  $\Delta\phi$ , are presented in Fig. 4. Additional cuts on the reconstructed  $ZZ$  invariant-mass have been introduced to optimise the signal measurement: for Higgs boson mass of 300 GeV the accepted mass range lies between 286 and 312 GeV. The efficiencies for  $ZZ$  events coming from decays of scalar, pseudoscalar higgs and non-resonant background are compared. The polar-angle distributions differ among these three classes of events, therefore significantly different acceptances are obtained. Understanding of this effect is crucial, as it can mimic a pseudoscalar type of distribution. For the first time such effect is taken into account in the analysis of the considered process.

In the following analysis, the reconstructed  $\Delta\phi$  values range from 0 to  $\pi$ , since we are not able to distinguish between quark and antiquark jet.

## 5 Analysis

For arbitrary values of model parameters  $\lambda$  and  $\Phi_{CP}$  we calculate the expected angular and invariant mass distributions for  $ZZ$  and  $W^+W^-$  events by convoluting the corresponding cross-section formula with the analytic photon-energy spectra CompAZ [8]. To take into account detector effects, we convolute this further with the function parameterising the invariant-mass resolution and the acceptance function containing the angular- and jet-selection cuts.<sup>2</sup> For the measurement of the event distributions in  $\Delta\phi$  and  $\zeta$  we introduce the additional cuts on the reconstructed  $ZZ$  invariant mass (for  $ZZ$  events) or on the reconstructed  $W^+W^-$  invariant mass as well as on the higgs-decay angle  $\Theta_{\mathcal{H}}$  (for  $W^+W^-$  events). The cuts were optimised for the smallest relative error in the signal cross-section measurement.

The expected precision in the measurements of the  $\Delta\phi$ - and of the  $\zeta$ -distributions, for  $\gamma\gamma \rightarrow ZZ \rightarrow l^+l^-jj$  events and  $\gamma\gamma \rightarrow W^+W^- \rightarrow 4j$  events is illustrated in Figs. 5 and 6, respectively. Calculations were performed for the primary electron-beam energy of 152.5 GeV and the Higgs-boson mass of 200 GeV. The results are compared with the expectation of the generic model with  $\Phi_{CP} = 0$  (as in SM) and  $\Phi_{CP} = \frac{\pi}{2}$ . For better comparison of the shape of distributions, results for pseudoscalar Higgs-boson couplings ( $\Phi_{CP} = \frac{\pi}{2}$ ) are normalised to the Standard Model expectations. We see, that even after taking into account beam spectra, detector effects, selection cuts and background influence, the differences between shapes of the angular distributions for the scalar and pseudoscalar couplings are still significant. Therefore we should be able to constrain Higgs-boson couplings from the shape of the distributions, even

---

<sup>2</sup>To simplify acceptance calculations, we neglect effects of the finite angular resolution.

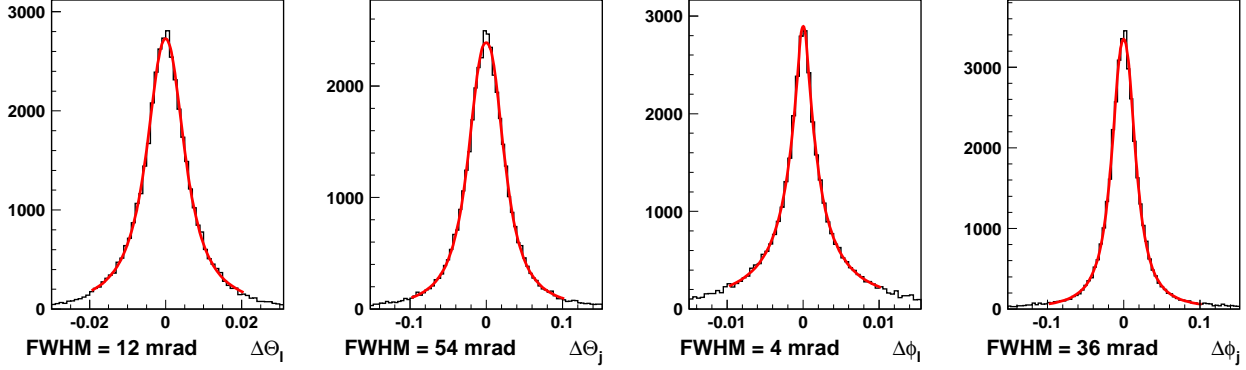


Figure 3: Resolution in the reconstructed  $Z$ -decay angles  $\Theta$  and  $\phi$ , for the leptonic ( $\Theta_l, \phi_l$ ) and hadronic ( $\Theta_j, \phi_j$ ) final states. Events were simulated with the PYTHIA and SIMDET programs, for a primary electron-beam energy of 209 GeV and Standard Model Higgs-boson mass of 300 GeV.

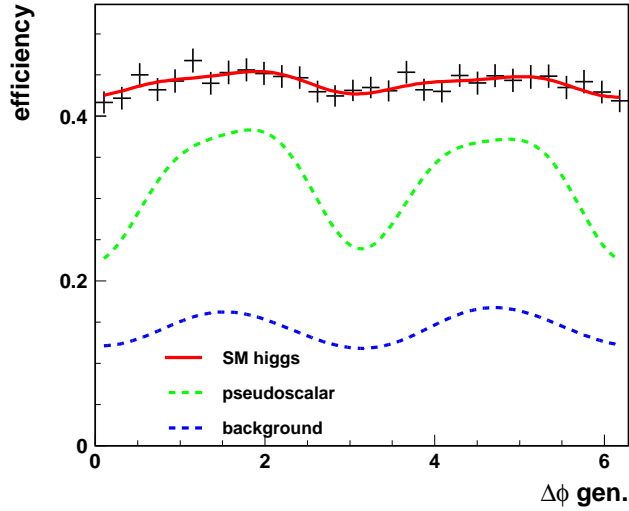


Figure 4: Selection efficiency as a function of the angle  $\Delta\phi$  between two  $Z$  decay planes, for  $ZZ \rightarrow l^+l^-jj$  events coming from the scalar higgs decays, pseudoscalar higgs decays and non-resonant background. Events were simulated with the PYTHIA and SIMDET programs, for a primary electron-beam energy of 209 GeV and Higgs-boson mass of 300 GeV. Only events with the reconstructed higgs mass between 286 and 312 GeV are accepted.

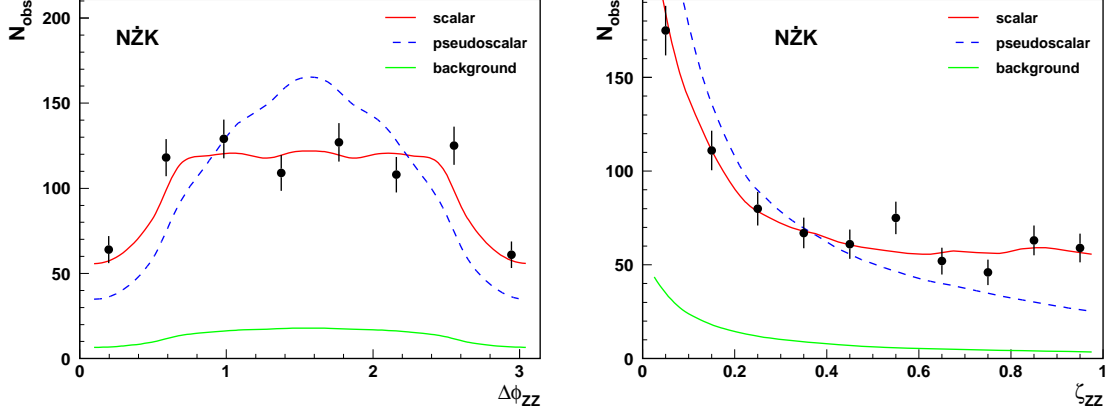


Figure 5: Measurement of the angle  $\Delta\phi_{ZZ}$  between two  $Z$ -decay planes (left plot) and of the variable  $\zeta_{ZZ}$  calculated from the polar angles of the  $Z \rightarrow l^+l^-$  and  $Z \rightarrow jj$  decays (right plot) for  $ZZ \rightarrow l^+l^-jj$  events. Points with error bars indicate the statistical precision of the measurement after one year of Photon Collider running at nominal luminosity. The solid (red) and dashed (blue) lines correspond to predictions of the model with pure scalar ( $\Phi_{CP} = 0$ ) and pseudoscalar ( $\Phi_{CP} = \frac{\pi}{2}$ ) Higgs-boson couplings, respectively. Green line represents the SM background of non-resonant  $ZZ$  production. Signal and background calculations are performed for primary electron-beam energy of 152.5 GeV and the Higgs-boson mass of 200 GeV.

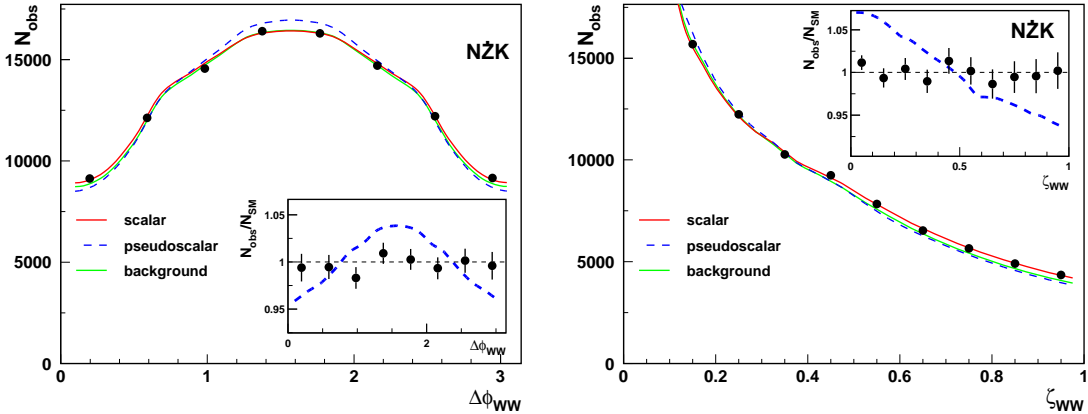


Figure 6: Measurement of the angle  $\Delta\phi_{WW}$  between two  $W$ -decay planes (left plot) and of the variable  $\zeta_{WW}$  calculated from the polar angles of two  $W \rightarrow jj$  decays (right plot) for  $WW \rightarrow 4j$  events. Points with error bars indicate the statistical precision of the measurement after one year of Photon Collider running at nominal luminosity. The solid (red) and dashed (blue) lines correspond to predictions of the model with pure scalar ( $\Phi_{CP} = 0$ ) and pseudoscalar ( $\Phi_{CP} = \frac{\pi}{2}$ ) Higgs-boson couplings, respectively. Green line represents the SM background of non-resonant  $W^+W^-$  production. Signal and background calculations are performed for primary electron-beam energy of 152.5 GeV and the Higgs-boson mass of 200 GeV. The insets show the relative deviations from the Standard Model predictions ( $\Phi_{CP} = 0$ ) for pseudoscalar Higgs-boson couplings.

if the overall normalisation related to the Higgs-boson production mechanism is not known. For the Standard-Model Higgs-boson decays to  $ZZ$ , about 675 Higgs-boson events and 145 non-resonant background events are expected after all selection cuts, in the selected mass window from 180 to 210 GeV. For the  $WW$  channel about 8000 signal events are expected, compared to about 170 000 background events. In both cases a statistical precision of the signal measurement is similar. However, due to overwhelming background contribution, the  $WW$  analysis is much more dependent on systematic uncertainties.

Each of the considered angular distributions discussed above can be fitted with model expectations, given in terms of the parameters  $\lambda$  and  $\Phi_{CP}$  describing Higgs-boson couplings to gauge bosons, parameters  $\Gamma_{\gamma\gamma}$  and  $\phi_{\gamma\gamma}$  describing the production mechanism, and an overall normalisation. Statistical errors in the determination of  $\Phi_{CP}$ , resulting from fits to the different distributions for  $ZZ$  events, are compared in Fig. 7. The remaining model parameters, except for the normalisation, are fixed to the Standard Model values. Out of the three considered angular distributions, parameter  $\zeta$  turns out to be the most sensitive to the angle  $\Phi_{CP}$  describing the CP-violation in the Higgs-boson couplings. Surprisingly, the smallest error is obtained from the fit to the invariant mass distribution. This is because, due to the different selection efficiencies for the scalar and pseudoscalar decays and also to interference effects, the relative normalisation of the Higgs-boson signal to the non-resonant background depends on the angle  $\Phi_{CP}$ . Therefore, we include the invariant mass distributions for  $W^+W^-$  and  $ZZ$  decays in the combined fit. When all parameters are allowed to vary in such a fit, the invariant-mass distributions constrain mainly the  $\Gamma_{\gamma\gamma}$  and  $\phi_{\gamma\gamma}$ .

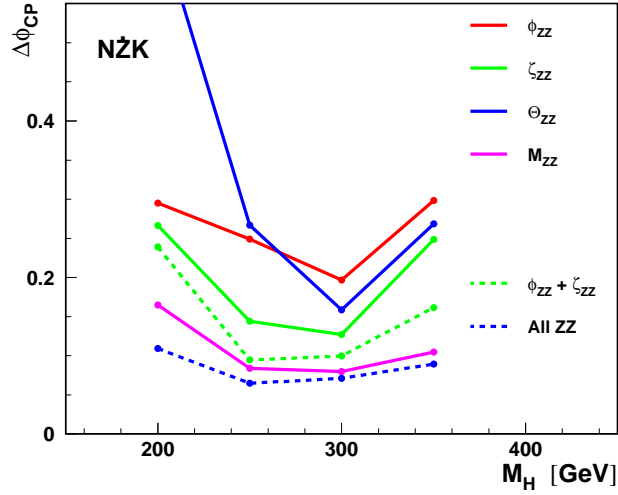


Figure 7: Statistical error in the determination of  $\Phi_{CP}$ , expected after one year of Photon Collider running, as a function of the Higgs-boson mass  $M_H$ . Fits were performed to the shape of the three individual angular distributions measured for  $ZZ$  events, as indicated in the plot, and to the reconstructed invariant mass distribution. Results of the simultaneous fits to three angular distributions and to all distributions are also shown. All other parameters, except for the overall normalisation, are fixed to the Standard Model values. Errors were calculated assuming  $\Phi_{CP} \approx 0$ .



## 6 Results

We calculate the expected statistical errors on the parameters  $\lambda$  and  $\Phi_{CP}$ , from the combined fit to angular distributions measured for  $ZZ$  and  $W^+W^-$  decays, and to the invariant mass distributions. Results are shown in Fig. 8. The two photon width of the Higgs boson,  $\Gamma_{\gamma\gamma}$ , the phase  $\phi_{\gamma\gamma}$  and normalisations of both samples are allowed to vary in the fit, so the results are independent of the production mechanism. One observes that for low Higgs-boson masses below 250 GeV, better constrains are obtained from the measurement of  $W^+W^-$  events, whereas for masses above 300 GeV smaller errors are obtained from the measurement of  $ZZ$  events. The error on  $\Phi_{CP}$  expected from the combined fit is below 50 mrad in the whole considered mass range. The corresponding error on  $\lambda$  is about 0.05.

## 7 Summary

An opportunity of measuring the Higgs-boson properties at the Photon Collider at TESLA has been studied in detail for masses between 200 and 350 GeV, using realistic luminosity spectra and detector simulation. We considered measurement of the invariant mass distributions and the various angular distributions. A new variable is proposed to describe the polar angle distributions of the secondary  $W^+W^-$  and  $ZZ$ -decay products. Event reconstruction and selection procedure result in acceptance corrections which are highly non-uniform and depend on the Higgs boson CP properties. Understanding of these effects is crucial in the analysis of angular distributions. From the model-independent study the angle describing a CP violation

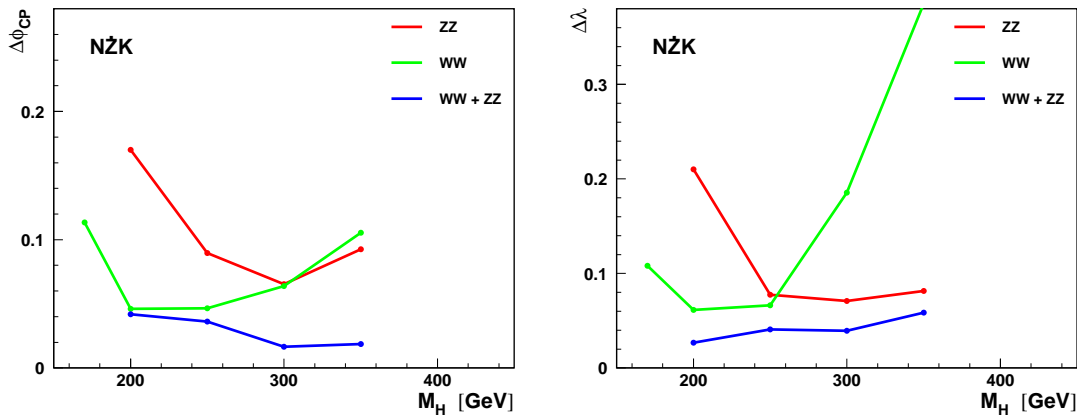


Figure 8: Statistical error in the determination of  $\Phi_{CP}$  (left plot) and  $\lambda$  (right plot), expected after one year of Photon Collider running, as a function of the Higgs-boson mass  $M_H$ . Combined fits were performed to the considered angular distributions and invariant mass distributions for  $ZZ$  events and  $W^+W^-$  events. Results were obtained assuming small deviations from Standard Model predictions, i.e.  $\lambda \approx 1$  and  $\Phi_{CP} \approx 0$ . Two photon width of the Higgs boson,  $\Gamma_{\gamma\gamma}$ , the phase  $\phi_{\gamma\gamma}$  and normalisations of both samples are allowed to vary in the fit.

in the generic Higgs-boson couplings to vector bosons can be determined with accuracy of about 50 mrad.

## Acknowledgements

We would like to thank our colleagues from the ECFA/DESY study groups for many useful comments and suggestions. This work was partially supported by the Polish Committee for Scientific Research, grant no. 1 P03B 040 26 and project no. 115/E-343/SPB/DESY/P-03/DWM517/ 2003-2005. P.N. acknowledges a partial support by Polish Committee for Scientific Research, grant no. 2 P03B 128 25. M.K. acknowledges a partial support by the European Community's Human Potential Programme under contract HPRN-CT-2000-00149 Physics at Colliders.

## References

- [1] B. Badelek et al., *Photon Collider at TESLA*, TESLA Technical Design Report, Part 6, Chapter 1, DESY-2001-011, ECFA-2001-209, DESY-TESLA-2001-23, DESY-TESLA-FEL-2001-05, March 2001, hep-ex/0108012.
- [2] P. Nieżurawski, A.F. Żarnecki, M. Krawczyk, JHEP 0211 (2002) 034 [hep-ph/0207294]
- [3] P. Nieżurawski, A.F. Żarnecki, M. Krawczyk, hep-ph/0403138.
- [4] P. Nieżurawski, A.F. Żarnecki, M. Krawczyk, ICHEP'2004, abstract #12-0740
- [5] D.J. Miller, S.Y. Choi, B. Eberle, M.M. Mühlleitner and P.M. Zerwas, Phys. Lett. B505 (2001) 149 [hep-ph/0102023]; S.Y. Choi, D.J. Miller, M.M. Mühlleitner and P.M. Zerwas, hep-ph/0210077; D.J. Miller, *Spin and Parity in the HZZ vertex*, presented at the ECFA/DESY meeting, Prague, November 2002.
- [6] E. Asakawa, K. Hagiwara, Eur. Phys. J. C31 (2003) 351; C.P. Buszello, I. Fleck, P. Marquard, J.J. van der Bij, Eur. Phys. J. C32 (2004) 209; C. P. Buszello, P. Marquard and J. J. van der Bij, hep-ph/0406181; M.T. Dova, S. Ferrari, hep-ph/0406313; R. M. Godbole, S. Kraml, M. Krawczyk, D. J. Miller, P. Nieżurawski and A. F. Żarnecki, hep-ph/0404024.
- [7] P. Nieżurawski, A.F. Żarnecki, M. Krawczyk, submitted to EPS'2003, July 17-23 2003, Aachen, Germany, abstract # 605; hep-ph/0307175.
- [8] A.F. Żarnecki, Acta Phys.Polon. B34 (2003) 2741 [hep-ex/0207021], <http://info.fuw.edu.pl/~zarnecki/compaz/compaz.html>
- [9] T. Sjostrand, P. Eden, C. Friberg, L. Lonnblad, G. Miu, S. Mrenna and E. Norrbin, *Comp. Phys. Comm.* 135 (2001) 238.
- [10] M. Pohl, H. J. Schreiber, DESY-99-030.